Seismic Source Spectrum of Tsunami and Ordinary Earthquake: A Quantitative Estimation of Tsunami from Forecoming Seismic Waves

Tôhoku Geophys. Journ. (Sci. Rep. Tôhoku Univ., Ser. 5), Vol. 29, No. 3, pp. 115–128, 1983

Seismic Source Spectrum of Tsunami and Ordinary Earthquakes: A Quantitative Estimation of Tsunami from Forecoming Seismic Waves

MASAYUKI TAKEMURA* and JUNJI KOYAMA

Geophysical Institute, Faculty of Science, Tohoku University,
Aramaki Aoba, Sendai, 980 JAPAN

(Received March 10, 1983)

Abstract: Spectral structure of earthquake sources are investigated analyzing earthquake magnitudes and seismic moment. About 3000 earthquakes from 1926 to 1978 are selected which occurred along the Kurile, Japan, and Ryukyu arcs from Seismological Bulletins of Japan Meteorological Agency. Earthquake magnitude by JMA, M_{JMA}, is determined from maximum amplitudes of seismic waves with a period of about 4 sec. Surface-wave magnitude, M_S, and body-wave magnitude, m_b, represent the amplitude of seismic waves with periods of 20 sec and 1 sec, respectively. M_S-M_{JMA} relation, therefore, provides us with information on the scaling of earthquake source-spectra, independent of the relation between M_S and m_b. Further analysis is made to consolidate the spectral structure introducing two new parameters; characteristic period, T_c, and seismic moment factor, M_e. T_c is shown to relate somehow to the period of corner frequencies and M_e to the seismic moment density at the period of T_c. Almost all earthquakes in the frontal arc regions show a coherent relation of M_e proportional to the cube of T_c, while earthquakes beneath the inner trench slopes show a different M_e-T_c relation. The latter earthquakes are classified into low-frequency earthquakes, because of longer T_c values than those of the former. Relations among earthquake magnitudes and seismic moment M_0, for the low frequency earthquakes are also different from those of the former earthquakes. Scaling models of earthquake source-spectra are constructed for ordinary earthquakes and low-frequency earthquakes, separately, taking into account the constraints of M_S-M_{JMA}, M_S-m_b, M_S-M_0, and M_e-M_0 relations. The last relation facilitates the estimation of seismic moment from M_e which can be evaluated through simple calculations. Tsunami magnitude estimated from a formula $m_{est}=1.3 \log M_0-34.9$, where M_0 is calculated from M_e, agrees quite well with that from tsunami wave heights in a wide dynamic range including low-frequency and ordinary earthquakes. This indicates that tsunami excitation can be quantitatively estimated from forecoming short-period seismic waves through the analysis of seismic moment factor and characteristic period of an earthquake.

1. Introduction

Earthquake source may be described simply as a time dependent release of stored strain energy due to a finitely-propagating fracture. The size and strength of earthquake sources have been expressed in terms of earthquake magnitudes. Surface-wave magnitude M_S has been introduced as such a scale using dominant amplitude of seismic surface-waves with a period of 20 sec at very long distances. Another scale widely

* Present Address: Building Engineering Department, Kajima Institute of Construction Technology, Tokyo, 182 Japan

used is body-wave magnitude m_b, which is defined based on amplitudes of seismic body waves with a period of about 1 sec. Therefore, M_S and m_b represent different parts of frequency spectrum of seismic sources.

Seismic moment M_0 is an alternative concept to estimate the size of earthquakes. The amplitude of seismic waves at a very long period is proporitional to $M_0=\mu DS$ (Aki, 1966), where S is fault area, D is average displacement discontinuity on the fault, and μ is rigidity at the source region. M_0 is, also, a parameter related to the total work done by an earthquake (Kanamori and Anderson, 1975).

It has been empirically studied the relations between tsunami energy and earthquake magnitude. However, the tsunami energy should be essentially compared to the total work done, and or seismic moment of earthquakes. Hatori (1979) studied a relation between seismic moment and tsunami magnitude m of tsunamigenic earthquakes, and obtained a simple relation;

$$\log M_0 = 0.77m+26.89\,. \tag{1}$$

This means, in turn, that tsunami magnitude and/or tsunami wave height can be estimated, if seismic moment of an earthquake is evaluated. Therefore, tsunami forecast may be precisely done through quick determination of seismic moment of earthquakes.

Seismic moment determination of an earthquake is very much complex not simple like earthquake magnitude determination. A method has been proposed by Koyama *et al.* (1982) to estimate seismic moment of earthquakes in a simple procedure but with sufficient accuracy. At first, we will give short summary of the method and study spectral structure of earthquake sources in wide magnitude range. Second, a quantitative estimation of tsunami wave heights will be made from amplitudes of short-period seismic waves.

2. Seismic Moment Factor and Characteristic Period

According to the studies on radiation patterns of seismic waves by Ben-Menahem (1961) and Hirasawa and Stauder (1965), the effect of finitely-propagating fracture on the amplitude radiation can be eliminated by taking a quantity of amplitude multiplied by its period. The quantity after correction of geometrical spreading and attenuation of seismic energy along the seismic ray-path is proportional to static seismic moment. This gives the basis of the present parameters to estimate seismic moments from tabulated data in usual seismological bulletins.

The materials necessary to the estimation are maximum amplitude of ground motions and its apparent period. The practical procedure is given as follows, taking the data on the Seismological Bulletins of the Japan Meteorological Agency (JMA). First, characteristic period T_c of an earthquake is introduced. Apparent periods of wavelets with maximum amplitudes in horizontal components for sample earthquakes are shown in Fig. 1 against epicentral distances. Remarkable feature in the figure is that a period of about 16 sec is predominant for epicentral distances longer than

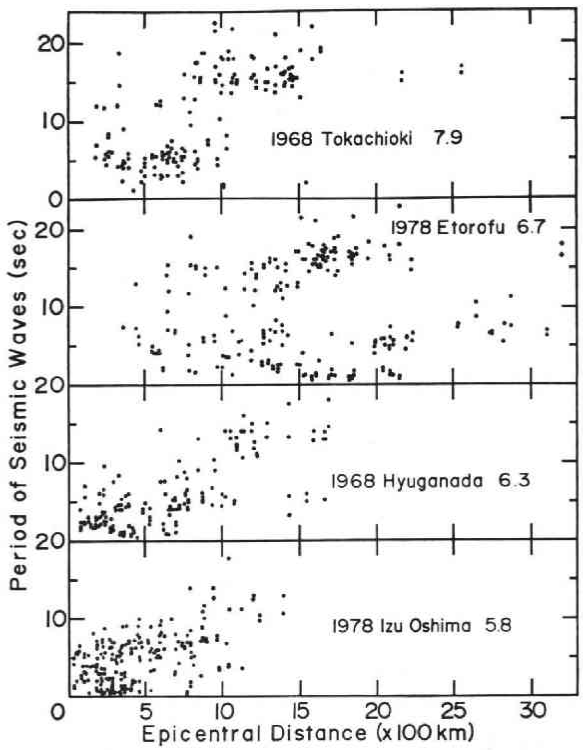

Fig. 1. Apparent period of seismic waves with maximum amplitude against epicentral distances. The data are quoted from Seismological Bulletins of Japan Meteorological Agency (JMA). Earthquakes are so selected as to cover various sizes and different locations. They are, from top to bottom, May 16, 1968 Tokachi-oki (M_{JMA}=7.9), March 23, 1978 Etorofu (M_{JMA}=6.7), April 1, 1968, Hyuganada (M_{JMA}=6.3), and January 15, 1978 Izu (M_{JMA}=5.8) earthquakes.

about 700 km. These wavelets are surface waves, presumably dispersed Rayleight waves (Koyama and Takemura, 1981). On the other hand, most of periods between 200 and 700 km in distance are scattered around 6 sec for the top trace and about 3 sec for the bottom trace in Fig. 1. The latter wavelets are considered to be S-waves, or reflected S-waves by some discontinuities.

The average period between 200 and 700 km in distance varies from one earthquake to another. We difine the characteristic period, T_c, of each earthquake by the average of apparent periods within the distance range from 200 to 700 km. This period may be somehow in relation to a time constant of earthquake source, the period of corner frequency which is commonly used to describe the seismic source spectrum.

Next, amplitude information is taken into consideration as another parameter. This parameter is defined as a product of maximum amplitude, its period and epicentral distance at each station. The multiplication of epicentral distance is understood to be a correction for the geometrical diminution, assuming wavelets in concern are of body-wave type. The average value is calculated from these products obtained from

horizontal components at stations within epicentral distances between 200 to 500 km, and the value is here designated as seismic-moment factor M_e at the period of T_c for a given earthquake. The dimension and absolute value of M_e thus calculated are different from those of seismic moment by some constant. The constant may be evaluated from elastic and unelastic constants at the source and along ray path, independent of the size and strength of earthquakes. The narrow range of distance, in comparison with that for T_c determination, is taken so as to reduce the uncertainty due to seismic energy attenuation into a permissible range and to obtain almost equal number of data for small earthquakes to that for large ones. The correction for the amplitude radiation pattern due to a fault geometry is assumed constant, because M_e is evaluated as an average of some tens of observations with various azimuths from the epicenter.

An assumption that the wavelets with maximum amplitude is of body waves is not serious in the final result. If the wavelet is of surface waves, the geometrical diminution factor should be square root of epicentral distance in calculating M_e. Even in such a case the relative value of M_e would not change more than 30%, because of the narrow range of epicentral distances for the data. Standard deviation of T_c for

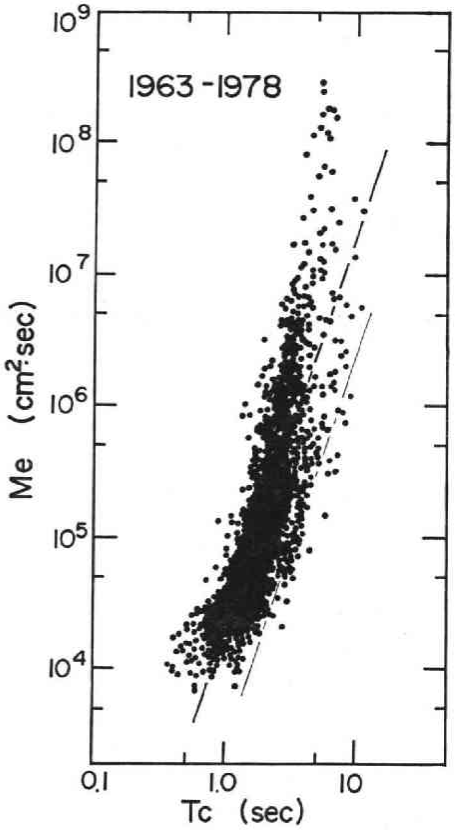

Fig. 2. Seismic-moment factor M_e and characteristic period T_c of earthquakes in and near Japan from 1963 to 1978. About 3000 earthquakes are analyzed of which surface-wave magnitude M_S covers the range from about 3.0 to 8.3. Dense solid line indicates general trend of M_e and T_c relation for small earthquakes and thin solid line the relation of a group apart from the trend. Both the lines represent the relation of $M_e \propto T_c^3$.

each earthquake is generally less than 1.5 sec, and uncertainty of M_e is mostly less than a factor of 2.0.

In the analysis of M_e and T_c, about 3000 shallow earthquakes are selected, which occurred along the Kurile, Japan, and Ryukyu arcs. Included are disastrous earthquakes from 1926 to 1962 and all earthquakes of which M_e's are calculated from 1963 to 1978. Surface-wave magnitude M_s of those earthquakes covers the range from 3 to 8.3.

Fig. 2 shows M_e and T_c for earthquakes from 1963 to 1978. The relation in Fig. 2 between M_e and T_c is well approximated by that M_e is proportional to the cube of T_c for earthquakes of which T_c is shorter than 5 sec. This suggests that the similarity relations among source parameters are valid for those earthquakes (Aki, 1967). This result would be a strong constraint for scaling earthquakes source spectra.

M_e for larger earthquake no longer falls on the line of cube of T_c. This is attributed to the instrumental response of the JMA seismographs. After the great Kwanto earthquake of 1923, the JMA established standardized seismological network using Wiechert seismographs. Electromagnetic seismographs having almost identical characteristics to Wiechert seismographs took place since early 1960's. Both seismographs have a natural period of about 5 sec, so that the instrumental characteristics distort the spectrum of ground motion especially in the period range longer than 5 sec. This will be again discussed with an illustration of seismic source spectra convolved with the instrumental characteristics.

Special interest is tens of earthquakes plotted in Fig. 2 which are meaningfully apart from the scatter of the data. It is also found that those earthquakes satisfy $M_e \propto T_c^3$ relation which is drawn in the figure. The period T_c is almost twice as long as that for ordinary earthquakes. T_c is an average value of apparent periods of seismic waves, so that those earthquakes are considered to be low-frequency earthquakes usually identified by visual inspection of seismograms (*e.g.*, Fukao and Kanjo, 1979).

The relation between M_e and T_c for low-frequency earthquakes is also a strong constraint to describe source spectra of low-frequency and tsunami earthquakes. Next, we will discuss the other constraints for scaling seismic source spectrum, showing the difference of earthquake sources between low-frequency and ordinary earthquakes.

3. Low-Frequency Earthquakes and Ordinary Earthquakes

Low-frequency earthquakes in Fig. 2 are small in magnitude compared to those previously found (Fukao and Kanjo, 1979; Utsu, 1980). A quantitative identification of low-frequency earthquakes may be done taking a parameter δ of seismic moment factor divided by the cube of characteristic period; $\delta = M_e/T_c^3$. Fig. 3 shows δ plotted on the epicenter of each earthquake with M_e smaller than 5×10^5 cm^2 sec. A smaller δ corresponds to a longer T_c, thus indicating low-frequency earthquakes.

Significant feature is that earthquakes with smaller δ mostly located in the inner trench slopes between curves A and B in Fig. 3, which are the traces of the Japan trench (or the Ryukyu, Izu-Bonin, Kurile trenches) and of the 3000 m bathymetric

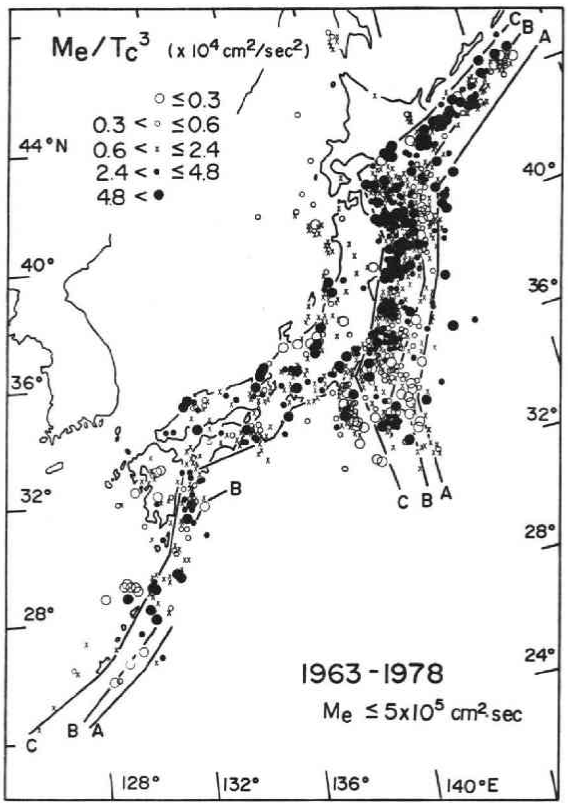

Fig. 3. Regional distribution of $\delta(=M_e/T_c^3)$ for earthquakes with M_e smaller than 5×10^5 cm² sec from 1963 to 1978. δ clearly shows the regional variation, which is bounded by curves A, B, and C. Curves A, B, and C correspond approximately to the trench axis, the 3000 m bathymetric depth, and the coast line of Japan islands. Region 1 is the lands and the marginal seas bounded by the curve C, region 2 is in between B and C, region 3 is in between A and B, and region 4 is oceanic side bounded by the trench axis A.

contour. Most of earthquakes, meanwhile, located between the curves of B and C, the latter of which is introduced to distinguish earthquakes in the crust from those along the subduction zone. The major trend of M_e-T_c relation in Fig. 2 is, therefore, for the earthquakes in this frontal arc region.

Relations among earthquake magnitudes and seismic moment for low-frequency earthquakes, M_S-M_{JMA}, M_S-m_b, and M_0-M_S relations, are also different from those for ordinary earthquakes, where M_{JMA} is earthquake magnitude by the Japan Meteorological Agency and it represents the logarithmic amplitude of seismic waves with a period of about 4 sec. Mutual relations among those earthquake magnitudes may be closely related to those among discrete spectra of earthquake sources at corresponding periods of magnitude definitions; say, M_S at 20 sec, m_b at 1 sec, and M_{JMA} at 4 sec, respectively. Figs. 4 a) and b) show M_S-M_{JMA} relations for ordinary earthquakes in the frontal arc regions and for low-frequency earthquakes in the inner trench slopes. On the average, an ordinary earthquake with M_S=5.5 measures

5.8 in M_{JMA} scale, on the other hand, a low-frequency earthquake does about 5.5. The difference is also obvious in the M_S-m_b relations between those two groups of earthquakes. Although the scatter of the data in Fig. 5 is very large, general trends of the data are different each other as much as 0.5 in m_b scale. The difference indicates that amplitude of short period seismic waves of a low-frequency earthquake is about three times smaller than that of an ordinary earthquake with the same value of surface-wave magnitude.

Scaling models of earthquake source spectra have been constructed (Takemura and Koyama, 1981) for ordinary and low-frequency earthquakes separately under the constraints mentioned above in addition to the result in Fig. 2. Solid curves in Fig. 6 indicate such a group of source spectra for ordinary earthquakes and dashed curves for low-frequency earthquakes. Detailed discussions on the source spectra were made elsewhere (Takemura and Koyama, 1981), however, an intuitive understanding on the source spectra is given as: There would be alternative understandings of source spectra for low-frequency earthquakes. One is that high frequency decay of source

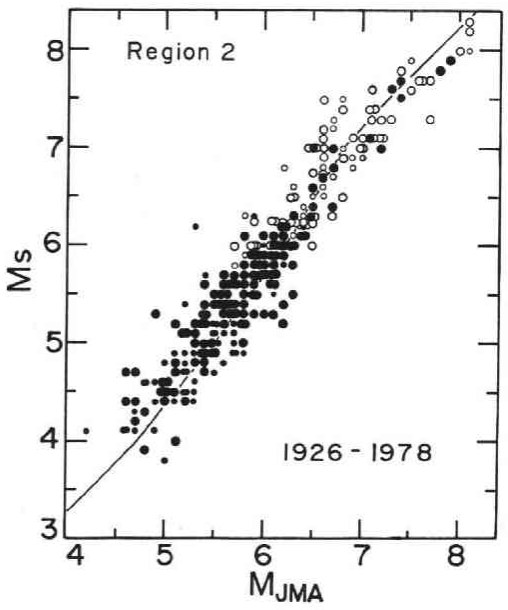

Fig. 4(a)

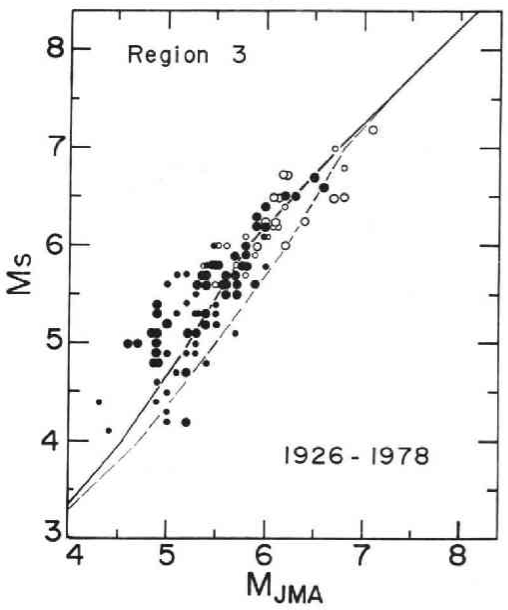

Fig. 4(b)

Fig. 4 a). Surface-wave magnitude M_S and JMA magnitude M_{JMA} of earthquakes in the subduction zones near Japan (region 2). Solid curve indicates the M_S-M_{JMA} relation theoretically calculated from the ordinary scaling model. Large and small open-circles indicate M_S's quoted from Gutenberg and Richter (1954) and those by Koyama and Takemura (1981), respectively. Solid circles indicate M_S's from the Earthquake Data Report by the USGS. Small solid circles indicate those determined from single station data.

b). Surface-wave magnitude M_S and JMA magnitude M_{JMA} of earthquakes in the inner trench slopes near Japan (region 3). Solid curve indicates the M_S-M_{JMA} relation theoretically calculated from the low-frequency model and broken curve is that from the ordinary scaling model. Other symbols are the same as those in Fig. 4 a).

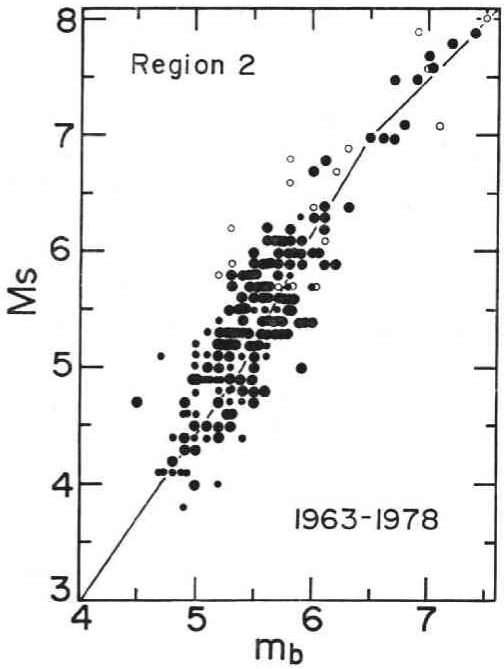

Fig. 5(a)

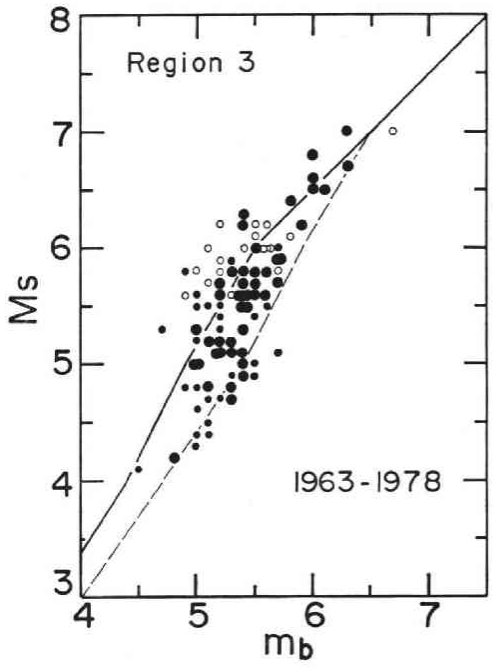

Fig. 5(b)

Fig. 5 a) Body-wave magnitude m_b and surface-wave magnitude M_S of earthquakes in the subduction zones near Japan (region 2). Solid curve indicates the m_b-M_S relation theoretically calculated from the ordinary scaling model. Other symbols are the same as those in Fig. 4 a).

b). Body-wave magnitude m_b and surface-wave magnitude M_S of earthquakes in the inner trench slopes near Japan (region 3) from 1963 to 1978. Solid curve indicates the m_b-M_S relation theoretically calculated from the low-frequency model and broken curve is that from the ordinary scaling model. Other symbols are the same as those in Fig. 4 a).

spectrum is larger for low-frequency earthquakes than that for ordinary earthquakes with the same value of seismic moment. Consequently, spectral content of low-frequency earthquakes in a short-period range is much less than that of ordinary earthquakes. The other is that corner frequency of source spectra is lower for low-frequency earthquakes than that for ordinary earthquakes with the same value of seismic moment, however, the high frequency decay of source spectra may be similar each other. All the constraints in the wide magnitude range favor the latter model, suggesting the difference of corner frequencies between low-frequency and ordinary earthquake sources with the same value of seismic moment is about 2 in factor. The low-frequency model of source spectra has settled the above debate, indicating the scaling relation among disastrous tsunami earthquakes and low-frequency earthquakes with small magnitudes, where tsunami earthquakes mean not merely tsunamigenic earthquakes but those generating tsunamis with large amplitudes disproportionate to their surface wave magnitudes.

The validity of the source spectra, as a first approximation, may be reconfirmed

comparing seismic moment and seismic moment factor of each earthquake. It is necessary to take into account the instrumental response of the JMA seismographs in order to directly compare the value of M_e's to that of seismic moments in Fig. 6. To do this, we assume seismic moment of the 1978 Miyagi-oki earthquake, 3×10^{27} dyne cm (Seno et al., 1980), matches M_e and T_e of the Miyagi-oki earthquake, 8.7×10^{7}cm^{2}sec and 4.0 sec. Fig. 7 shows M_e's and source spectra multiplied by the instrumental response so adjusted. It is seen that M_e's are consistent with the peak values of the

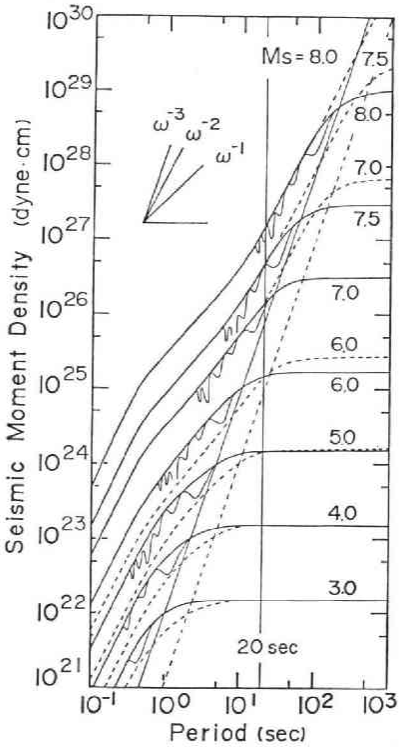

Fig. 6.

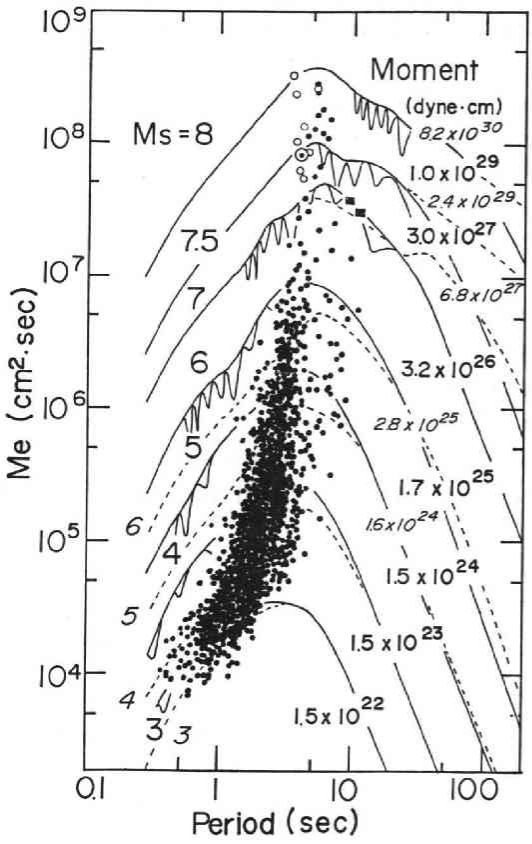

Fig. 7.

Fig. 6. Scaling models of earthquake source-spectra. Solid curves indicate the ordinary scaling model and dotted curves the low-frequency model. Solid and dotted curves represent the relation that seismic moment M_0 is proportional to the cube of period of corner frequency. The value of M_S should be read along the line at 20 sec.

Fig. 7. Seismic-moment factor M_e and characteristic period T_c of earthquakes in and near Japan. Open circles indicate the results of major earthquakes from 1926 to 1962 of which M_S's are larger than about 7.5. Solid circles are the same as those in Fig. 2. Low-frequency (tsunami) earthquakes identified are plotted by squares, which are the 1963 and 1975 Kurile earthquakes. Solid and dotted curves represent the theoretical source spectra from the ordinary scaling and the low-frequency models multiplied by the frequency characteristics of the JMA electromagnetic seismograph. Double circle indicates the Miyagi-oki earthquake of 1978 (M_{JMA}=7.4), which is used to scale the relation between M_e and M_0.

spectra and those for smaller earthquakes fall on a line which is inversely proportional to the cube of corner frequencies. This is also the same for low-frequency earthquakes. The largest low-frequency earthquakes are the 1963 and 1975 Kurile earthquakes which are plotted by squares in Fig. 7. These earthquakes are identified to be tsunami earthquakes from detailed analyses of long-period body-waves and mantle Rayleigh waves (Takemura et al., 1977; Takemura, 1977). Although seismic moment factors of the 1963 and 1975 Kurile earthquakes are smaller than that of the Miyagi-oki earthquake; the reference event, the characteristic periods are by far long, manifesting the difference between ordinary and tsunami earthquakes.

Once the adjustment between M_e and M_0 has been made, it is possible to estimate M_0 of any earthquakes from M_e through this figure. This may be justified in comparing seismic moment estimated in this manner from seismic moment factors with that evaluated from amplitude of seismic waves through conventional analyses. Static seismic moments of 27 earthquakes among all the events in this study have been determined independently by the conventional analyses of near- and far-field seismic observations. Fig. 8 shows seismic moments of those earthquakes together with estimated seismic moments in this study. The figure demonstrates that most of the present results fall in the range of uncertainty of the conventional analyses, which is approximately taken to be a factor of 3. Tsunami earthquakes, low-frequency earthquakes with large magnitudes, are also analyzed and plotted in Fig. 8. The seismic moment of the 1963 and 1975 Kurile earthquakes is in fairly good agreement with that estimated based on the low-frequency model. The essential difference of the

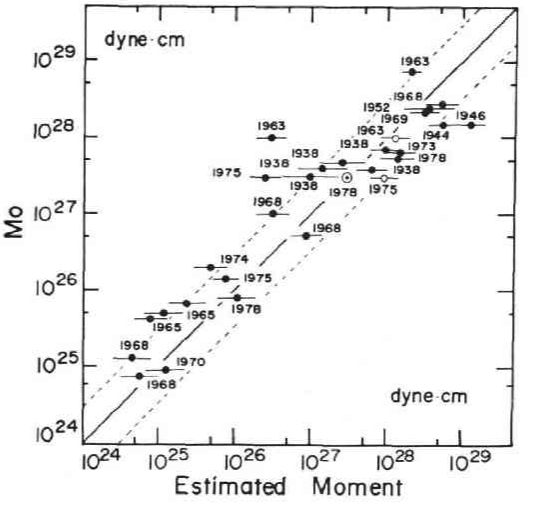

Fig. 8. Seismic moment M_0 and that estimated from seismic moment factor M_e of earthquakes in and near Japan. Solid circles indicate the estimated M_0 by using the ordinary scaling model. Open circles indicate those by using the low-frequency model, which are calculated only for the earthquakes in region 3. Broken lines represent the uncertainty of seismic moment determination by the conventional methods being assumed to be a factor of 3. The length of bars attached to each event indicate the uncertainty of the present analysis.

present method from that estimating seismic moment through earthquake magnitudes is that the characteristic period is taken into account for the estimation. Short-period seismographs, acting as a high-pass filter, are sometimes very sensitive to the difference of amplitude spectra like as we see in Fig. 7. Because M_e of an earthquake may be evaluated without laborious calculations, the estimation of seismic moment in the present manner has high potential for the routine processing of seismic data, especially for the tsunami forecast or the tsunami warning system.

4. Estimation of Tsunami from Seismic Waves

The relation of eq. (1) or its inverse as

$$m = 1.3 \log M_0 - 34.9 \qquad (2)$$

is applicable in a wide dynamic range of seismic moments approximately from 10^{26} to 3×10^{30}dyne·cm (Hatori, 1979) not only to tsunamigenic earthquakes but also to tsunami earthquakes. Tsunami magnitude has been originally introduced by Imamura (1949) and Iida (1956) to measure the intensity or the strength of tsunamis generated by earthquakes near Japan. The unity of this tsunami magnitude is reduced to the twofold wave-height of maximum tsunamis. And the magnitude underflows at −1 which corresponds to maximum tsunami wave-height less than 50 cm. There are 78 earthquakes in and near Japan which generated tsunamis in the time from

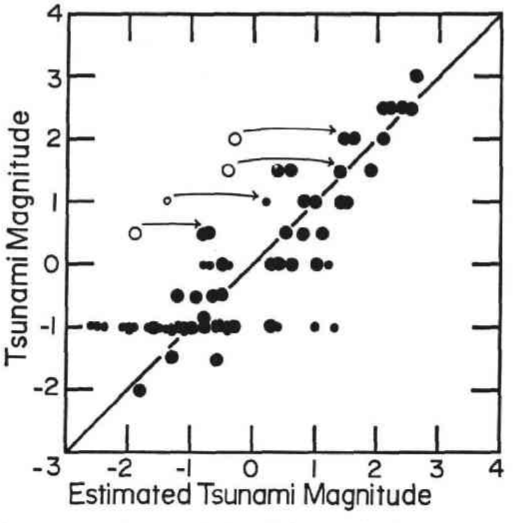

Fig. 9. Tsunami magnitudes and those calculated from seismic moments which are estimated from seismic moment factor M_e. Large symbols indicate redetermined values of tsunami magnitude by Hatori (1971, 1979), and small symbols are quoted from Usami (1975). Open circles are those identified to be low-frequency (tsunami) earthquakes. When the low-frequency model is used for these earthquakes, estimated tsunami magnitudes are by far large indicated by the pointing of arrows. Lower limit, −1, is obvious for tsunami magnitudes by Usami (1975). Scattering of the data seems to be large, however, the standard deviation of the regression line in the figure is about 0.6. This uncertainty is corresponding to the uncertainty of tsunami wave height by a factor of 1.5.

1926 to 1981 (Watanabe, 1968; Usami, 1975; Hatori, 1969, 1971, 1979). Small circles in Fig. 9 show tsunami magnitudes in the original definition, meanwhile large circles indicate those redetermined by Hatori (1971, 1979) taking into account the geometrical diminution of tsunami wave-heights.

Seismic moments of the 78 earthquakes are estimated from seismic moment factors and their tsunami magnitudes are calculated using eq. (2). The values are plotted in Fig. 9 against tsunami magnitudes evaluated from actual observations of tsunami wave-heights. Open symbols in Fig. 9 indicate tsunami earthquakes of the 1963 and 1975 Kurile earthquakes and the 1938 Ryukyu and the 1947 West Hokkaido earthquakes being discriminated by their characteristic periods. Their tsunami magnitudes are re-evaluated based on the low-frequency model and are plotted by symbols in Fig. 9 pointed by arrows. Estimated tsunami magnitudes are consistent with those from tsunami wave-heights in a wide dynamic range. Least squares regression of a straight line gives about 0.6 as the standard deviation of the present estimations. This is corresponding to the uncertainty in tsunami wave-heights of 1.5 in a factor. It should be emphasized again that characteristic periods play an important role to discriminate low-frequency earthquakes; tsunami earthquakes, out of substantial ordinary earthquakes and to measure tsunami excitations from relatively short-period seismic waves.

5. Summary of Conclusions

Seismic-moment factor M_e and characteristic period T_c have been calculated for about three thousand earthquakes in and near Japan. It has been found in the M_e and T_c diagram that M_e is proportional to the cube of T_c for samall earthquakes. This implies that the similarity relations among source parameters are valid for those earthquakes. M_e and T_c diagram also revealed that there is a group of earthquakes of which M_e and T_c relation is meaningfully different from general trend of the data. These earthquakes correspond to low-frequency earthquakes identified through visual inspection of seismograms by Fukao and Kanjo (1980) along the northern part of Japan trench. The present analysis demonstrates that low-frequency earthquakes are commonly found in the inner trench slopes of the Japan, Ryukyu, Izu-Bonin and Kurile trenches, although the activity of them is much less than that of ordinary earthquakes along the frontal arc regions. It has been very difficult in the framework of studies to investigate the low-frequency nature of earthquake sources through visual inspection of seismograms. The relation between M_e and T_c and those among earthquake magnitudes suggest the similarity rule among low-frequency earthquakes with small magnitudes and disastrous tsunami earthquakes.

The scaling models of earhquake source spectra have been presented for ordinary and low-frequency earthquakes. An empirical relation between seismic moment factor M_e and static seismic moment M_0 has been obtained, and seismic moment of any earthquake can be quickly estimated from the relative value of M_e's by using the source spectra for the ordinary and the low-frequency models. Characteristic period T_c has

been shown to be a sensitive parameter in discriminating low-frequency earthquakes, and it plays the key role to evaluate tsunami exciations from forecoming seismic waves.

Earthquake magnitudes are calculated only from maximum amplitude of seismice waves. Seismograms of low-frequency earthquakes show long-period nature of source dynamics being quite different from those of ordinary earthquakes. Seismic moment of such earthquakes is much different from that of ordinary earthquakes, even though earthquake magnitudes are the same. Being a product of amplitude and period of seismic waves, M_e is easily related to the amplitude spectrum of eathquake sources, distinguishing low-frequency nature of earthquakes. Because the period of tsunami waves is very long, it is necessary to take into account the long-period nature of earthquake sources in the estimation of tsunami excitations. The present approach is to evaluate seismic moment relatively to that of a standard earthquake, which is essentially the same way as to determine earhquake magnitudes, however, there are two kind of constants corresponding to low-frequency and ordinary earthquakes.

References

Aki, K., 1966, Generation and propagation of G waves from the Niigata earthquake of June 16, 1964, Bull. Earthq. Res. Inst., **44**, 73–88.

Aki, K., 1967, Scaling law of seismic spectrum, J. Geophys., Res., **72**, 1217–1231.

Ben-Menahem, A., 1961, Radiation of seismic surface-waves from finite moving sources, Bull. Seism. Soc. Am., **51**, 401–435.

Fukao, Y. and K. Kanjo, 1979, A zone of low-frequency earthquakes beneath the inner wall of the Japan trench, Tectonophysics, **67**, 153–162.

Gutenberg, B., aud C.F. Richter, 1954, *Seismicity of the earth and associated phenomena,* Prinston Univ. Press, 2nd ed., 310 pp.

Hatori, T., 1969, Dimensions and geographic distribution of tsunami sources near Japan, Bull. Earthq. Res. Inst., **47**, 185–214.

Hatori, T., 1971, Tsunami sources in Hokkaido and southern Kurile regions, Bull. Earthq. Res. Inst., **49**, 63–75.

Hatori, T., 1979, Relation between tsunami magnitude and wave energy, Bull. Earthq. Res. Inst., **54**, 531–541 (in Japanese with English abstract).

Hirasawa, T. and W. Stauder, S.J., 1965, On the seismic body waves from a finite moving source, Bull. Seism. Soc. Am., **52**, 237–262.

Iida, K., 1956, Earthquakes accompanied by tsunami occurring under the sea off the isolands of Japan, J. Earth Sci., Nagoya Univ., **4**, 1–43.

Imamura, M., 1949, Catalog of tsunami in Japan, Zisin II, **2**, 23–28 (in Japanese).

Kanamori, H. and D.L. Anderson, 1975, Theoretical basis of some empirical relations in seismology, Bull. Seism. Soc. Am., **65**, 1073–1095.

Koyama, J. and M. Takemura, 1981, Quantification of earthquakes and tsunami prediction, Abst. Seism. Soc. Japan, **1981 No. 1**, 158 (in Japanese).

Koyama, J., M. Takemura, and Z. Suzuki, 1982, A scaling model for quantification of earthquakes in and near Japan, Tectonophyscis, **84**, 3–16.

Seno, T., K. Shimazaki, P. Sommerville, K. Sudo, and T. Eguchi, Rupture process of the Miyagi-oki, Japan, earthquakes of June 12, 1978, Phys. Earth Planet. Inter., **23**, 39–61.

Takemura, M., 1977, Source process of tsunami earthguakes in Kurile Islands region, a thesis submitted to Tohoku Univ., 80 pp.

Takemura, M. and J. Koyama, 1981, Seismic source spectrum of tsunami and ordinary earthquakes, Abst. Internat. Tsunami Symp., IUGG, 1–4.

Takemura, M., J. Koyama, and Z. Suzuki, 1977, Source process of the 1974 and 1975

earthquakes in Kurile islands in special relation to the difference in excitation of tsunami, Sci. Rep. Tohoku Univ., Ser. **5**, Geophys., **24**, 113–132.

Usami, T., 1975, *Descriptive table of disastrous earthquakes in Japan*, Univ. Tokyo Press, 1–327 (in Japanese).

Utsu, T., 1980, Spatial and temporal distribution of low-frequency earthquakes in Japan, J. Phys. Earth, **28**, 361–384.

Watanabe, H., 1968, Descriptive table of tsunamis in and near Japan, Zisin II, **21**, 293–313 (in Japanese).